Analysis of the Robustness of FMT Modulation in Time-Frequency Selective Fading Channels

Andrea M. Tonello and Francesco Pecile

DIEGM - Università di Udine - Via delle Scienze 208 - 33100 Udine - Italy
phone: +39 0432 558 042 - fax: +39 0432 558 251 - e-mail: tonello@uniud.it

Abstract— In this paper we analyze the performance of Filtered Multitone (FMT) modulation systems in time-frequency selective fading channels. FMT generalizes the OFDM scheme through the deployment of a sub-channel shaping pulse. A general analysis framework is presented, and it is specialized to the case of using a root-raised cosine pulse (FMT) and a rectangular pulse (OFDM). Quasi-closed form expressions for the signal-to-interference (SIR) power ratio are derived. The results allow to benchmark the multitone system and understand how robust it is to frequency selective time-variant fading. An analysis both in terms of SIR and bit-error-rate is made. It is shown that the better sub-channel spectral containment of the FMT yields better performance than OFDM.

***Index Terms*—DMT modulation, FMT modulation, fast fading, frequency selective fading, OFDM.**

I. INTRODUCTION

In this paper we analyze the performance of Filtered Multitone (FMT) modulation in time-variant frequency selective fading channels. FMT is a discrete-time implementation of multicarrier modulation that uses uniformly spaced sub-carriers and identical sub-channel pulses [1]. Orthogonal Frequency Division Multiplexing (OFDM) (also referred to as Discrete Multitone Modulation (DMT)) can be viewed as an FMT scheme that deploys rectangular time domain filters [2]. FMT has been originally proposed for application in broadband wireline channels [1], and subsequently it has been investigated for application in wireless channels [3].

The main research problems related with FMT are the efficient digital implementation, the design of the prototype pulse, the development of equalization schemes, and in general the performance analysis. A popular efficient polyphase filter bank architecture has been proposed by Cherubini et al. in [1]. The channel time-frequency selectivity may introduce inter-carrier interference (ICI) and ISI that can be minimized with the design of optimal time-frequency confined pulses [4]-[5]. Simplified sub-channel equalizers have been devised in [3]. Although multitone systems are robust to channel frequency selectivity, they are sensitive to carrier frequency offsets and phase noise, as well as to fast time variations of the channel impulse response [6]-[7]. An extensive literature exists on the performance analysis of multicarrier systems in time-variant frequency selective fading channels. However, most of this work focuses on the OFDM solution where fast fading introduces ICI [8], while dispersive fading introduces both ICI and ISI when the cyclic prefix is shorter than the channel duration [7], [9]. In [10] we have studied the performance limits of FMT modulation, and we have shown that FMT can provide both frequency and time diversity gains when optimal multi-channel equalization is used. However, if complexity is an issue, it is likely that linear single channel equalizers are used. In this case the ICI can limit the performance. A performance comparison between FMT and OFDM has been done in [11]. In our paper, we provide a more general framework to the analysis of the SIR power ratio in FMT systems over time-variant frequency selective fading channels. The SIR can also be used to predict the bit-error-rate (BER) performance of FMT and OFDM with single tap sub-channel equalization.

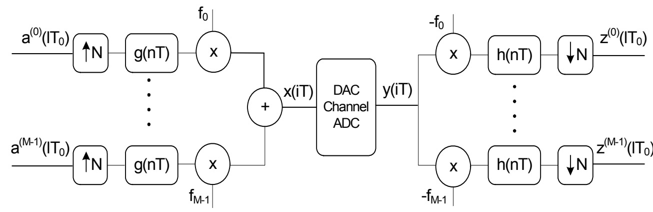

Fig.1. FMT transmission system.

This paper is organized as follows. In Section II the system model is described and we evaluate the output of the receiver filter bank when transmission is over a time-variant frequency selective channel. In Section III, the average power of the signal and interference components is derived. We discuss the results and we report a comparison with OFDM in Section IV with reference to the SIR performance, and in Section V with reference to the BER performance. Finally, the conclusions follow.

II. FMT MODULATION SCHEME

An FMT modulation based architecture is depicted in Fig.1 where we assume the following system parameters[1]: T is the transmission period; $W = 1/T$ is the transmission bandwidth; M is the number of sub-channels; $T_0 = NT$ is the sub-channel symbol period; $f_k = k/MT$ is the k-th sub-carrier; $g(nT)$ is the prototype pulse; $R = M/T_0$ is the overall transmission rate in symbol/s. The transmitter (synthesis stage) generates the signal

[1] T is assumed to be the time unit. $\mathrm{rect}(t) = 1$ for $0 \le t < 1$, and zero otherwise. $rep_F(.)$ denotes the periodic repetition with period F.

Proceedings of IEEE Vehicular Technology Conference Fall 2007
Baltimore - USA - September 30 - October 3, 2007

$$x(iT) = \sum_{k=0}^{M-1} \sum_{l \in \mathbb{Z}} a^{(k)}(lT_0) g(iT - lT_0) e^{j2\pi f_k iT} \qquad i \in \mathbb{Z} \quad (1)$$

where $a^k(lT_0)$ is the sequence of complex data symbols, e.g., M-QAM, that is transmitted on sub-channel $k = 0,...,M-1$ at rate $1/T_0$. A frequency guard equal to $f_G = 1/MT - 1/NT$ exists between sub-channels if the prototype pulse has confined frequency response with bandwidth $1/T_0$.

In this paper we specialize the analysis of performance for the following prototype pulse:

$$g(nT) = \text{rrcos}\left(\frac{nT}{T_0}\right), \quad G(f) = T_0 rep_{1/T}\left\{\text{RRCOS}(fT_0)\right\}, \quad (2)$$

where $\text{rrcos}(t)$ denotes the impulse response of a root-raised cosine pulse with roll-off factor α, and $\text{RRCOS}(f)$ is the Fourier transform of the pulse [8].

It is interesting to note that (1) allows to represent also a cyclically prefixed (CP) OFDM signal when we fix the sub-carrier spacing at $1/MT$, and we define the prototype pulse as $g(nT) = \text{rect}\left(nT/T_0\right)$.

A. Receiver Filter bank Output

The signal (1) is digital-to-analog converted and transmitted over the communication channel (after RF conversion). The received lowpass signal is analog-to-digital converted to obtain $y(iT)$, and then it is passed through an analysis filter bank with prototype pulse $h(nT)$. The sampled output at rate $1/T_0$ corresponding to sub-channel k is

$$z^{(k)}(lT_0) = \sum_{i \in \mathbb{Z}} y(iT) e^{-j2\pi f_k iT} h(lT_0 - iT). \quad (3)$$

In FMT the analysis pulse is matched to the synthesis pulse, i.e., $h(nT) = g^*(-nT)$. In CP-OFDM the analysis pulse is $h(nT) = \text{rect}\left(-nT/MT\right)$ with $MT \le T_0 = (\mu + M)T$. Using this analysis pulse corresponds to discard the cyclic prefix of length μ samples at the beginning of the received block. Note that in CP-OFDM there is a sub-channel SNR penalty equal to M/N compared to FMT due to a receiver pulse that is not matched to the transmit pulse [10].

We model the baseband channel with a discrete-time time-variant filter $g_{CH}(nT;mT)$ that comprises the effect of the DAC and ADC stages

$$g_{CH}(nT;mT) = T \sum_{p \in \mathrm{P}} \alpha_p(nT) \delta(mT - pT), \quad (4)$$

where $\delta(mT - pT)$ is a discrete-time Dirac delta equal to $1/T$ for $m = p$, and zero otherwise. Assuming wide sense stationary scattering, the time-variant tap amplitudes $\alpha_p(nT)$, $p \in \mathrm{P} \subset \mathbb{Z}$, can be modeled as stationary complex Gaussian processes [8]. Further, with the Clarke's isotropic scattering model [8], the tap amplitudes have zero mean, and correlation

$$r_{p,p'}(nT) = E\left[\alpha_p(mT)^* \alpha_{p'}(mT + nT)\right] = \Omega_{p,p'} J_0(2\pi f_D nT), \quad (5)$$

where $\Omega_{p,p'} = E\left[\alpha_p(mT)^* \alpha_{p'}(mT)\right]$, while f_D is the maximum Doppler, and $J_0(t)$ denotes the zero order Bessel function of the first kind [12]. Correlation among the T-spaced channel taps can be introduced by the filters in the ADC stage [8], [10]. The Delay Doppler Spread Power Spectrum is obtained by the Fourier transform of (5) and it is equal to [8]

$$\begin{gathered} R_{p,p'}(f) = rep_{1/T}\left\{\hat{R}_{p,p'}(f)\right\} \\ \text{with } \hat{R}_{p,p'}(f) = \frac{\Omega_{p,p'}}{\pi f_D \sqrt{1 - (f/f_D)^2}} \quad |f| < f_D, \quad 0 \ \textit{otherwise}. \end{gathered} \quad (6)$$

It follows that the k -th sub-channel filter-bank output reads

$$z^{(k)}(lT_0) = \sum_{\hat{k}=0}^{M-1} \sum_{m=-\infty}^{\infty} a^{(\hat{k})}(mT_0) g_{EQ}^{(\hat{k},k)}(lT_0; mT_0) + \eta^{(k)}(lT_0) \quad (7)$$

where $\eta^{(k)}(lT_0)$ is the Gaussian noise contribution, while the equivalent impulse response between the input sub-channel $\hat{k}$, and output sub-channel k is defined as

$$\begin{aligned} g_{EQ}^{(\hat{k},k)}(lT_0; mT_0) = e^{j2\pi(f_{\hat{k}} mT_0 - f_k lT_0)} \sum_{i=-\infty}^{\infty} h^{(k)}(lT_0 - iT) \\ \times \sum_p \alpha_p(iT) g^{(\hat{k})}(iT - pT - mT_0). \end{aligned} \quad (8)$$

In (8) we use the frequency shifted transmit and receive pulses that are defined respectively as

$$g^{(k)}(nT) = g(nT) e^{j2\pi f_k nT}, \ h^{(k)}(nT) = h(nT) e^{j2\pi f_k nT}. \quad (9)$$

Therefore, the output in the absence of noise can be written as

$$z^{(k)}(lT_0) = a^{(k)}(lT_0) g_{EQ}^{(k,k)}(lT_0; lT_0) + ISI^{(k)}(lT_0) + ICI^{(k)}(lT_0) \quad (10)$$

where the first term represents the useful data contribution, the second additive term is the ISI contribution, the third term is the ICI contribution.

III. Analytical Evaluation of the Interference

We note that the sub-channel sequence of samples at the receiver output can be written as

$$z^{(k)}(lT_0) = \sum_{\hat{k}=0}^{M-1} z^{(\hat{k},k)}(lT_0) + \eta^{(k)}(lT_0) \quad (11)$$

where

$$z^{(\hat{k},k)}(lT_0) = \sum_{m=-\infty}^{\infty} a^{(\hat{k})}(mT_0) g_{EQ}^{(\hat{k},k)}(lT_0; mT_0) \quad (12)$$

is the contribution of the data stream transmitted on sub-channel $\hat{k}$ to the sub-channel analysis filter output of index k. We assume the data symbols to be i.i.d. with zero mean, and average power $M_a^{(k)} = E\left[|a^{(k)}(mT_0)|^2\right]$. Then, the average power of (12) equals

$$M_z^{(\hat{k},k)} = E[|z^{(\hat{k},k)}(lT_0)|^2] = M_a^{(\hat{k})} \sum_m E\left[\left|g_{EQ}^{(\hat{k},k)}(lT_0; mT_0)\right|^2\right], \quad (13)$$

where the second equality holds with independent zero mean data symbols. The computation is independent of the time instant lT_0 because we are in stationary conditions. We refer to (13) as the *cross power* since it is the power of the interference on sub-channel k that is generated by sub-channel $\hat{k}$. With the tapped delay line channel model, the cross power is

$$M_z^{(\hat{k},k)} = M_a^{(\hat{k})} \sum_m \sum_{p,p'} \sum_{i,i'} r_{p,p'}(iT) g^{(\hat{k})}(iT + i'T - pT + lT_0 - mT_0) \times h^{(k)}(-iT - i'T) g^{(\hat{k})*}(i'T - p'T + lT_0 - mT_0) h^{(k)*}(-i'T). \quad (14)$$

It should be noted that if we fix $\hat{k} = k$ in (14), and we isolate the term that corresponds to $m = l$, we obtain the sub-channel signal power $S^{(k)} = M_a^{(k)} E\left[| g_{EQ}^{(k,k)}(lT_0; lT_0) |^2 \right]$. The sum of all other terms yields the ISI power $M_{ISI}^{(k)} = E\left[| ISI^{(k)}(lT_0) |^2 \right]$, while the total power of the ICI can be obtained as $M_{ICI}^{(\hat{k})} = \sum_{\hat{k} \neq k} M_z^{(\hat{k},k)}$.

To proceed, we define the following *sub-channel product function*

$$gh^{(\hat{k},k)}(iT; sT) = g^{(\hat{k})}(iT - sT) h^{(k)}(-iT). \quad (15)$$

Then, we can rewrite (14) as

$$M_z^{(\hat{k},k)} = \frac{M_a^{(\hat{k})}}{T} \sum_m \sum_{p,p'} \sum_i r_{p,p'}(iT) c_{gh}^{(\hat{k},k)}(iT; sT, s'T) \quad (16)$$

where the deterministic autocorrelation of the sub-channel product function (15) is defined as

$$c_{gh}^{(\hat{k},k)}(iT; sT, s'T) = T \sum_{i'} gh^{(\hat{k},k)}(iT + i'T; sT) gh^{(\hat{k},k)*}(i'T; s'T). \quad (17)$$

The expression (16) is quite general, but it can be detailed for a certain choice of the sub-channel pulses. In certain cases, depending on the prototype pulse and the channel, it is convenient to calculate the cross power (16) partially in the frequency domain using the formula

$$M_z^{(\hat{k},k)} = \frac{M_a^{(\hat{k})}}{T} \sum_m \sum_{p,p'} \sum_i r_{p,p'}(iT) \int_{-1/2T}^{1/2T} C_{gh}^{(\hat{k},k)}(f; sT, s'T) e^{j2\pi fiT} df, \quad (18)$$

or in the frequency domain with the following formula that is obtained via the Parseval theorem

$$M_z^{(\hat{k},k)} = \frac{M_a^{(\hat{k})}}{T^2} \sum_m \sum_{p,p'} \int_{-1/2T}^{1/2T} R_{p,p'}(-f) C_{gh}^{(\hat{k},k)}(f; sT, s'T) df. \quad (19)$$

In (18)-(19) we use the discrete-time Fourier transform $C_{gh}^{(\hat{k},k)}(f; sT, s'T) = T \sum_n c_{gh}^{(\hat{k},k)}(nT; sT, s'T) e^{-j2\pi fnT}$. This transform can be written as

$$C_{gh}^{(\hat{k},k)}(f; sT, s'T) = GH^{(\hat{k},k)}(f; sT) GH^{(\hat{k},k)*}(f; s'T) \quad (20)$$

where $GH^{(\hat{k},k)}(f; sT)$ is the discrete-time Fourier transform of the product function (15), i.e.,

$$GH^{(\hat{k},k)}(f; sT) = rep_{1/T}\left[\left(G^{(\hat{k})}(f) e^{-j2\pi fsT} \right) * H^{(k)}(-f) \right], \quad (21)$$

and $G^{(k)}(f)$, $H^{(k)}(f)$ are the Fourier transforms of the frequency shifted pulses in (9). In the FMT scheme the receiver filter-bank is matched to the transmitter filter-bank, therefore, $H^{(k)}(f) = G^{(k)*}(f)$.

In the following we specialize the results when the prototype pulse is root-raised cosine and rect. Further, we consider the channel to exhibit uncorrelated scattering so that the channel taps are statistically independent with zero mean, and power $\Omega_p = E[| \alpha_p(iT) |^2]$. This assumption is accurate as the signal bandwidth gets wide. It allows to simplify the analysis and acquire insights about the system performance. Data symbols with equal power, $M_a^{(k)} = M_a$, are also considered. Since we are in stationary conditions we evaluate the SIR for $l = 0$. With these assumptions the signal-to-interference power ratio (SIR) is the same over all sub-channels. When the channel taps are correlated the average SIR may vary across sub-channels as, for instance, shown in [10]. However, such a variation is small for typical wide band channels.

IV. SIR Evaluation

The results in the previous section allow the evaluation of the SIR power ratio on sub-channel k

$$SIR^{(k)} = \frac{S^{(k)}}{M_{ISI}^{(k)} + M_{ICI}^{(k)}}. \quad (22)$$

To compute (22) we need to numerically solve some integrals, e.g., the one in (19). This can be done by deriving equivalences that are obtained via series expansions [12]. To gain insight and distinguish between the effect of the delay spread and the Doppler spread, we consider first a multipath channel with quasi-static fading, and then a time-variant flat fading channel. Finally, we discuss the effects of a joint time and frequency selective fading channel. The multipath channel is assumed to have power delay profile Ω_p with N_P independent taps. Further, we assume identical signal power on all sub-channels. With these assumptions, the SIR is independent of the sub-channel index.

A. Frequency Selective Static Fading Channel

Let us assume the channel to be quasi-static but frequency selective. Then, it is possible to elaborate further (16), and obtain simple expressions for the signal and interference power in FMT. We report them in Appendix. In Fig.2.A, we show the SIR as a function of the normalized delay spread γ for the FMT system. We assume an exponential delay profile $\Omega_p \sim e^{-pT/(\gamma T)}$, and we truncate the channel at -20 dB. We fix the number of sub-channels $M = 32$ and we set the factor $N = 40$. It should be noted, that the delay spread is γT such that if the transmission bandwidth is 1 MHz, it equals $8\ \mu s$ for $\gamma = 8$.

The figure shows that the FMT architecture is robust to channel frequency selectivity. When the delay spread γ gets larger, the power of the ISI increases, thus the SIR decreases. It can be counteracted by using a higher number of sub-carriers (thus obtaining narrower sub-channels) or, if the SIR is particularly low, by using a sub-channel equalizer. In the case of CP-OFDM, the power of the useful term, the ISI and the ICI are computed from (16) and reported in Appendix. Now, comparing the curves in Fig.2.A, we can see that for small delay spreads CP-OFDM has better SIR performance than FMT, because the ISI is handled by the CP. However, as the delay spread increases and the channel becomes longer than the CP, OFDM also exhibits SIR floors. For instance, the

SIR difference between OFDM and FMT is only 3 dB for $\gamma = 4$.

B. Flat Fast Fading

Now, let us assume the channel to be flat but time-variant. We start this section discussing the results of Fig.2.B where we plot the SIR as a function of normalized Doppler $f_D T$. The curves start from $f_D T = 2\times 10^{-6}$. With bandwidth of 1 MHz the Doppler equals 50 Hz when $f_D T = 5\times 10^{-5}$.

Comparing the curves in Fig.2.B we see that OFDM performs significantly worse than FMT with the r.r.c. pulse. In this case FMT exhibits 30 dB gain at $f_D T = 0.4\times 10^{-4}$ over OFDM. It should be noted that the autocorrelation of the r.r.c. pulse is no more an ISI free pulse in the presence of large Doppler, so that ISI is present and it lowers the SIR.

C. Joint Time and Frequency Selective Fading Channel

The joint effect of the time and frequency channel selectivity is illustrated in Fig.3. The SIR is plotted as a function of the normalized delay spread γ for several values of maximum Doppler $f_D T$. It shows that the SIR for OFDM remains constant as the CP is longer than the channel. Further, FMT has superior SIR performance for $\gamma < 1.5$ as a result of being more robust to channel time variations. Then, the two systems have similar performance. For the parameters herein considered, the effect of the delay spread dominates for $\gamma > 1.5$, while for $\gamma < 1.5$ is the Doppler spread that lowers the SIR.

V. BER ANALYSIS

The SIR analysis of the previous section allows to predict the BER performance when single tap sub-channel equalization is used. That is, with the Gaussian approximation for the interference, and, for instance with 4-PSK modulation, the BER on sub-channel k can be approximated as follows [8]

$$BER^{(k)} = \frac{1}{2} - \frac{1}{2}\sqrt{\frac{1}{2}\left(\frac{1}{SIR^{(k)}} + \frac{1}{SNR^{(k)}}\right)^{-1}}. \tag{23}$$

We report in Fig.4 a comparison between the theoretical BER (23), and the one that is obtained via Monte Carlo simulation.

We show the BER as a function of the signal-to-noise ratio for various values of normalized delay spread γ (with the same channel profile of Section IV.A) and several values of normalized Doppler $f_D T$. We consider a 32 sub-channels FMT system with a r.r.c pulse with roll-off 0.2, and with $N = 40$. We consider OFDM with 32 tones and a CP of length 8. 4-PSK modulation is used. The two systems have identical data rate and deploy a single tap equalizer. The figure shows that in OFDM the theoretical and simulated curves are very close, while for FMT the discrepancy is more pronounced. This is due to the fact that in OFDM the Gaussian approximation is more accurate because a large number of intercarrier and intersymbol terms adds up to generate the interference.

As the SIR analysis has already shown, single tap equalization in FMT is sufficient for $\gamma < 1.5$ and smaller losses than in OFDM are experienced as the Doppler spread increases. For $\gamma = 1.5$ the performance of FMT is dominated by the channel frequency selectivity while OFDM by the time selectivity. For $\gamma > 1.5$, high error floors are exhibited by both systems although are more pronounced in OFDM.

VI. CONCLUSIONS

We have presented an analysis of the effect of time and frequency selectivity in FMT modulation schemes. We have obtained quasi-closed form expressions for the signal-to-interference power ratio. The results allow to characterize the effect of fading channels in these systems as a function of the Doppler-delay spread. The frequency confinement of the sub-channels makes the FMT scheme robust to the inter-carrier interference that can be generated by the channel time and frequency selectivity. Some ISI can arise but it can be handled with sub-channel equalization. In fast Rayleigh fading, FMT with a root-raised-cosine prototype pulse and a simple one tap equalizer has superior SIR performance than OFDM. In frequency selective fading they have similar performance.

VII. APPENDIX

A. Results in Frequency Selective Fading

When the channel is quasi-static but frequency selective with independent channel taps, we can obtain the following expressions for the signal and interference power in FMT

$$S_{FMT}^{(k)} = M_a \sum_{p=0}^{N_P} \Omega_p \left|k_g(-p)\right|^2 \tag{24}$$

$$M_{ISI-FMT}^{(k)} = M_a \sum_{m\neq 0}\sum_{p=0}^{N_P} \Omega_p \left|k_g(-mN-p)\right|^2 \tag{25}$$

where the prototype pulse autocorrelation is equal to

$$k_{\mathrm{rrcos}}(p) = N\,\mathrm{rcos}\left(\frac{p}{N}\right). \tag{26}$$

In (26) $\mathrm{rcos}(t)$ denotes the impulse response of a raised cosine filter. The ICI power is always zero assuming that the sub-carrier spacing is larger than $(1+\alpha)/T_0$.

For the frequency selective static fading channel herein considered, we obtain the following expressions for OFDM

$$S_{OFDM}^{(k)} = M_a\left(\sum_{p=0}^{\min(N-M,N_p)} \Omega_p M^2 + \sum_{p=N-M+1}^{\min(N-1,N_p)} \Omega_p (N-p)^2\right), \tag{27}$$

$$\begin{aligned} M_{OFDM-ISI}^{(k)} = M_a \sum_{m\neq 0}\sum_{p=0}^{N_p}\Omega_p \sum_{i=0}^{M-1}\sum_{i'=0}^{M-1} \mathrm{rect}\left(\frac{iT+mT_0+pT}{T_0}\right) \\ \times \mathrm{rect}\left(\frac{i'T+mT_0+pT}{T_0}\right), \end{aligned} \tag{28}$$

$$\begin{aligned} M_{OFDM-ICI}^{(k)} = M_a \sum_{m}\sum_{p=0}^{N_p}\Omega_p \sum_{i'=0}^{M-1}\left[\mathrm{rect}\left(\frac{i'T+mT_0+pT}{T_0}\right)\right. \\ \left.\times\left(M - \sum_{i=0}^{M-1}\mathrm{rect}\left(\frac{iT+mT_0+pT}{T_0}\right)\right)\right]. \end{aligned} \tag{29}$$

In (28)-(29) the sum in m has a finite number of terms depending on the channel duration. When the channel is shorter than the CP, i.e., $N_p \le \mu = N - M$, the useful power is $S^{(k)} = M_a M^2 \sum_{p=0}^{N_P} \Omega_p$, while the ISI and ICI are zero. The formulas (27)-(29) give the power of the signal and the interference when the channel is longer than the CP [8].

B. *Results in Fast Flat Fading*

In the following we report the analytical results that have been used to plot the curves in Fig.2.B and that are derived under the assumption of fast flat fading with the Clarke's scattering model.

With the r.r.c pulse, the signal power and the power of the ISI term have a complex expression that is a combination of Bessel and Struve functions [12]. They are omitted for space limitations. The power of the ICI cannot be computed in closed form. However, $M_{FMT-ICI}^{(k)}$ is zero if the sub-channels are separated by more than the maximum Doppler.

For the CP-OFDM system the power of the useful term and the ICI can be found

$$S_{OFDM}^{(k)} = M_a \Omega_0 \sum_{i=0}^{M-1} \sum_{i'=0}^{M-1} J_0(2\pi f_D T(i-i')), \tag{30}$$

$$M_{OFDM-ICI}^{(k)} = M_a \Omega_0 \left(M^2 - \sum_{i=0}^{M-1} \sum_{i'=0}^{M-1} J_0(2\pi f_D T(i-i')) \right). \tag{31}$$

The total power of the ISI is always zero. Note that (31) is identical to the one reported in [8].

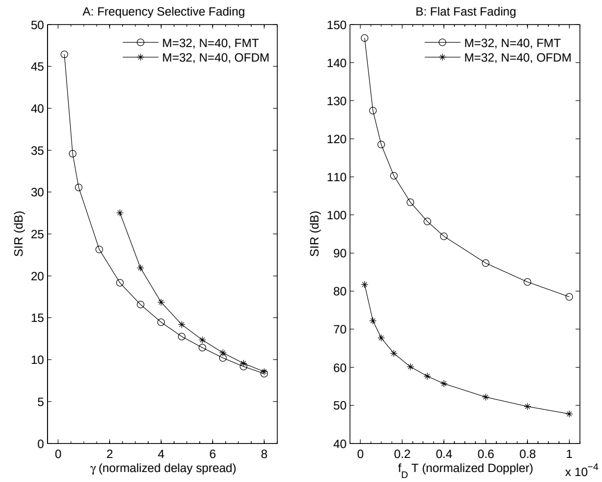

Fig. 2. SIR performance as a function of delay spread in frequency selective fading and as a function of maximum Doppler in fast fading. FMT with root-raised-cosine pulse and OFDM.

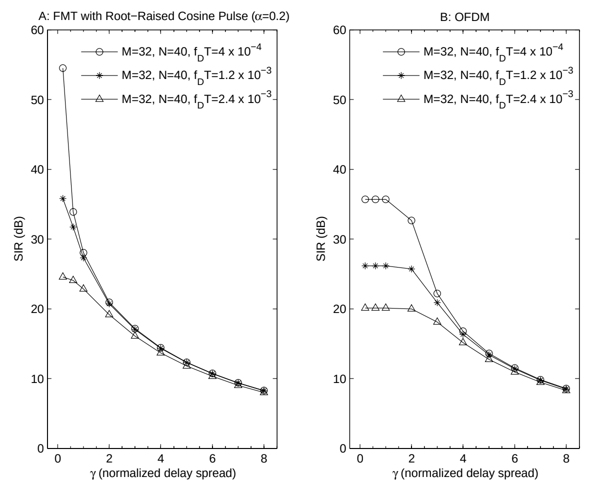

Fig. 3. SIR performance in a joint time-frequency selective fading channel. FMT with root-raised-cosine pulse and OFDM.

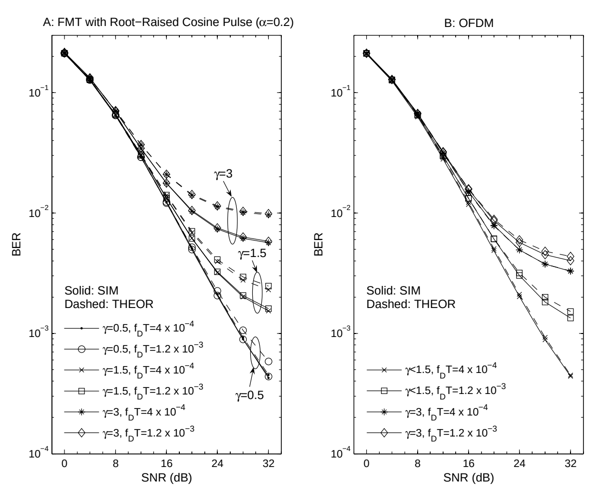

Fig.4. BER for several values of maximum Doppler and delay spread. FMT with root-raised-cosine pulse and OFDM with cyclic prefix. The systems have M=32 and N=40. Both theoretical and simulated curves are shown.

REFERENCES

[1] G. Cherubini, E. Eleftheriou, S. Ölçer, "Filtered multitone modulation for very high-speed digital subscriber lines," *IEEE Journal on Select. Areas in Comm.*, pp. 1016-1028, June 2002.

[2] J.A.C. Bingham, "Multicarrier Modulation for data Transmission, an Idea whose Time Has Come," *IEEE Comm. Magazine*, vol. 31, pp. 5-14, May 1990.

[3] N. Benvenuto, S. Tomasin, L. Tomba, "Equalization methods in DMT and FMT systems for broadband wireless communications," *IEEE Trans. on Comm.*, vol. 50, pp. 1413-1418, Sept. 2002.

[4] W. Kozek, A. F. Molisch, "Nonorthogonal pulseshapes for multicarrier communications in doubly dispersive channels," *IEEE Journal on Select. Areas in Comm.*, vol. 16, pp. 1579-1589, Oct. 1998.

[5] T. Strohmer, S. Beaver, "Optimal OFDM design for time-frequency dispersive channels", *IEEE Trans. on Comm.*, vol.51, pp. 1111-1122, July 2003.

[6] L. Tomba, W. A. Krzymien, "Effect of carrier phase noise and frequency offset on the performance of multicarrier CDMA systems," *Proc. of IEEE ICC 96, Dallas,* pp. 1513-1517, June. 1996.

[7] M. Speth, S. A. Fetchel, G. Fock, H. Meyr, "Optimum receiver design for wireless broad-band systems using OFDM – Part I," *IEEE Trans. on Comm.*, vol. 47, no. 11, pp 1668-1677, Nov. 1999.

[8] G. L. Stuber, Principles of Mobile Communications, Kluwer, 1996.

[9] H. Steendam, M. Moeneclaey, "Analysis and Optimization of the Performance of OFDM on Frequency-Selective Time-Selective Fading Channels," *IEEE Trans. on Comm.*, vol.47, pp. 1811-1819, Dec. 1999.

[10] A. Tonello, "Performance limits for filtered multitone modulation in fading channels," *IEEE Trans. on Wireless Comm.*, vol. 4, pp. 2121-2135, Sept. 2005.

[11] T. Wang, J. G. Proakis, and J. R. Zeidler, "Interference Analysis of Filtered Multi-tone Modulation over Time-Varying Fading Channels," in *Proc. of the IEEE Global Comm. Conf.*, vol. 6, St. Louis, pp. 3586-3591, Nov. 2005.

[12] M. Abramowitz, I. Stegun, *Handbook of Mathematical Functions*, Dover Publ., New York, 1970.